Severely Impaired B Lymphocyte Proliferation, Survival, and Induction of the c-Myc:Cullin 1 Ubiquitin Ligase Pathway Resulting from CD22 Deficiency on the C57BL/6 Genetic Background

Jonathan C. Poe, Karen M. Haas, Junji Uchida, Youngkyun Lee, Manabu Fujimoto and Thomas F. Tedder

J Immunol 2004; 172:2100-2110; ;
doi: 10.4049/jimmunol.172.4.2100
http://www.jimmunol.org/content/172/4/2100

The Journal of Immunology is published twice each month by
The American Association of Immunologists, Inc.,
1451 Rockville Pike, Suite 650, Rockville, MD 20852

Print ISSN: 0022-1767 Online ISSN: 1550-6606.

Severely Impaired B Lymphocyte Proliferation, Survival, and Induction of the c-Myc:Cullin 1 Ubiquitin Ligase Pathway Resulting from CD22 Deficiency on the C57BL/6 Genetic Background[1]

Jonathan C. Poe, Karen M. Haas, Junji Uchida, Youngkyun Lee, Manabu Fujimoto,[2] and Thomas F. Tedder[3]

Understanding the molecular mechanisms through which CD22 regulates B lymphocyte homeostasis, signal transduction, and tolerance is critical to defining normal B cell function and understanding the role of CD22 in autoimmunity. Therefore, CD22 function was examined in vivo and in vitro using B cells from CD22-deficient ($CD22^{-/-}$) mice. Backcrossing of founder $CD22^{-/-}$ mice onto the C57BL/6 (B6) genetic background from a B6/129 mixed background resulted in a dramatically reduced B cell proliferative response following IgM ligation, characterized by a paucity of lymphoblasts and augmented apoptosis. Also, the phenotype of splenic B6 $CD22^{-/-}$ B cells was uniquely HSA^{high} and $IgD^{low}/CD21^{low}$ with intermediate levels of CD5 expression, although the percentages of mature and transitional B cells were normal. That B6 $CD22^{-/-}$ B cells predominantly underwent apoptosis following IgM ligation correlated with this unique tolerant phenotype, as well as defective induction of the c-Myc:Cullin 1 (CUL1) ubiquitin ligase pathway that is necessary for progression to the S phase of cell cycle. CD40 ligation compensated for CD22 deficiency by restoring lymphoblast development, proliferation, c-Myc and CUL1 expression, and protein ubiquitination/degradation in IgM-stimulated B6 $CD22^{-/-}$ B cell cultures. Thereby, this study expands our current understanding of the complex role of CD22 during B cell homeostasis and Ag responsiveness, and reveals that the impact of CD22 deficiency is dictated by the genetic background on which it is rendered. Moreover, this study defines CD22 and CD40 as the first examples of lymphocyte coreceptors that influence induction of the c-Myc:CUL1 ubiquitin ligase pathway. ***The Journal of Immunology*****, 2004, 172: 2100–2110.**

Understanding the molecular mechanisms that regulate B lymphocyte homeostasis and tolerance is critical to defining normal B cell function and identifying alterations that lead to humoral autoimmune disease (1–3). Cell surface receptors that modulate homeostatic and B cell Ag receptor (BCR)[4]-mediated signals provide a context for normal B cell responses to foreign Ags, while preserving tolerance and preventing aberrant responses that lead to the production of self-reactive Abs (4). Among these receptors is CD22, a B cell-restricted transmembrane glycoprotein that serves as a cell surface adhesion molecule through its extracellular Ig-like domains (5–8). B cells express CD22 as they mature in the bone marrow to acquire positive signaling responses via surface IgM (9). Following IgM or CD22 ligation, conserved tyrosine residues within the CD22 cytoplasmic domain become phosphorylated at augmented levels (10–12), including tyrosines within consensus immunoreceptor tyrosine-based inhibition motifs (5, 8). The net effect of CD22 phosphorylation at these sites is the recruitment of potent intracellular phosphatases and the negative regulation of IgM-induced signals (6, 13–15). As a consequence, B cells from $CD22^{-/-}$ mice exhibit exaggerated intracellular calcium responses following IgM ligation and have a high in vivo turnover rate, which results in reduced numbers of circulating B cells (16–21). Moreover, CD22 deficiency ($CD22^{-/-}$) on either the C57BL/6 (B6) or BALB/c genetic backgrounds results in high-affinity, isotype-switched autoantibody production (22).

The finding that tyrosine-phosphorylated CD22 recruits positive signaling molecules has suggested that CD22 may also carry out positive regulatory roles (8, 23–26). In addition, stimulation of splenic B cells from two lines of $CD22^{-/-}$ mice generated on B6/129 mixed genetic backgrounds using optimal concentrations of $F(ab')_2$ anti-IgM Abs results in reduced B cell proliferation relative to wild-type B cells (18, 19). To date, the apparently divergent negative and positive effects of CD22 deficiency on B cell signaling and proliferation following IgM ligation have remained unexplained. To address this issue further, we have examined $CD22^{-/-}$ B cell function in greater detail following IgM ligation, including analysis of cell cycle regulatory proteins. We have found that the cell surface phenotype and response to IgM stimulation of B6 $CD22^{-/-}$ B cells was remarkably different than for B cells from founder B6/129 $CD22^{-/-}$ mice. B6 $CD22^{-/-}$ B cells were

Department of Immunology, Duke University Medical Center, Durham, NC 27710

Received for publication July 24, 2003. Accepted for publication December 8, 2003.

The costs of publication of this article were defrayed in part by the payment of page charges. This article must therefore be hereby marked *advertisement* in accordance with 18 U.S.C. Section 1734 solely to indicate this fact.

[1] This work was supported by National Institutes of Health R01 Grants CA081776 and CA096547, and a grant from the Arthritis Foundation.

[2] Current address: Department of Regenerative Medicine, Research Institute, International Medical Center of Japan, Tokyo, Japan.

[3] Address correspondence and reprint requests to Dr. Thomas F. Tedder, Department of Immunology, Box 3010, Duke University Medical Center, Durham, NC 27710. E-mail address: thomas.tedder@duke.edu

[4] Abbreviations used: BCR, B cell Ag receptor; CUL1, Cullin 1; HSA, heat stable Ag; PI, propidium iodide; FSC, forward scatter; SHP, Src homology 2 domain-containing phosphotyrosine phosphatase; DNP-KLH, 2,4,-DNP-keyhole lympet hemocyanin; 7AAD, 7-aminoactinomycin D; PNA, peanut agglutinin; MZ, marginal zone; ERK, extracellular signal-regulated kinase; JNK, c-jun N-terminal kinase; SCF, Skp1-Cullin-F-box; PI 3-kinase, phosphatidylinositol 3-kinase; RT, room temperature; DPBS, Dulbecco's PBS.

0022-1767/04/$02.00

much more refractory to IgM-induced proliferation, characterized by impaired lymphoblast development, augmented cell death, and a defect in induction of the c-Myc:Cullin 1 (CUL1) ubiquitin ligase pathway that is necessary for progression to the S phase of the cell cycle (27). As such, these data expand our current understanding of the complex role CD22 plays in regulating B cell maturation, homeostasis, and Ag responsiveness, and defines CD22 as an important lymphocyte coreceptor that regulates the c-Myc:CUL1 ubiquitin ligase pathway.

Materials and Methods

Mice

B6/129 CD22$^{-/-}$ mice were as described (19), or were backcrossed at least eight times onto the B6 genetic background (B6 CD22$^{-/-}$). Wild-type littermates of each genetic background served as controls. Mice were 8–12 wk of age when used and were housed in a specific pathogen-free barrier facility. All studies and procedures were approved by the Duke University Animal Care and Use Committee (Durham, NC).

Abs and immunofluorescence analysis

Abs used in these studies included: F(ab′)$_2$ of goat anti-mouse IgM Abs (Cappel; ICN Biomedicals, Costa Mesa, CA); FITC-, PE-, or biotin-conjugated Abs against mouse heat stable Ag (HSA; clone M1/69), B220 (clone RA3-6B2), CD5 (clone 53-7.3), CD23 (clone B3B4), and CD21 (clone 7G6) (BD PharMingen, San Diego, CA); FITC-conjugated I-A/I-E MHC class II (clone M5/114.15.2; TIB120; American Type Culture Collection, Manassas, VA); hamster IgM anti-mouse CD40 Abs (clone HM40-3, no azide/low endotoxin (NA/LE) format; BD PharMingen); PE-conjugated rat anti-mouse IgD (clone 11-26) and FITC-conjugated polyclonal goat anti-mouse IgM (Southern Biotechnology Associates, Birmingham, AL); polyclonal rabbit antiserum reactive with phosphatidylinositol 3-kinase (PI 3-kinase) (Upstate Biotechnology, Lake Placid, NY); purified polyclonal rabbit Abs reactive with the phosphorylated and nonphosphorylated forms of Akt and Bad (New England Biolabs, Beverly, MA); purified rabbit polyclonal Abs reactive with Src homology 2 domain-containing phosphotyrosine phosphatase (SHP)-1 (Upstate Biotechnology, Lake Placid, NY); FITC-conjugated polyclonal goat anti-rabbit IgG (TAGO, Burlingame, CA); mouse mAb reactive with IκBα phosphorylated at serine 32 (B-9; Santa Cruz Biotechnology, Santa Cruz, CA); rabbit polyclonal Abs reactive with c-Myc (C-19), CUL1 (H-213), ubiquitin (FL-76), extracellular signal-regulated kinase (ERK)2 (C-14), p27^{Kip1} (C-19), and p21^{Waf1} (C-19) (Santa Cruz Biotechnology); HRP-conjugated polyclonal goat anti-rabbit IgG and anti-mouse IgG secondary Abs (Jackson ImmunoResearch Laboratories, West Grove, PA). Streptavidin-CyChrome secondary reagent was from BD PharMingen.

Single cell suspensions of tissue leukocytes were stained at 4°C using predetermined optimal concentrations of each test Ab for 20 min as described (28). Flow cytometry analysis was performed on a FACScan flow cytometer using the CellQuest program (BD Biosciences, San Jose, CA), as described (19).

Proliferation and apoptosis in B cell cultures

Spleen B cells were purified (>94% B220$^+$) from single cell suspensions by removing T cells with anti-Thy1.2 Ab-coated magnetic beads (Dynal, Lake Success, NY). B cells were resuspended in RPMI 1640 culture medium containing 10% FCS, 10 mM HEPES, and 55 μM 2-ME and cultured (2×10^5 cells in 0.2 ml of medium/well) in triplicate in 96-well flat-bottom tissue culture plates at 37°C with 5% CO_2 in the presence of F(ab′)$_2$ anti-IgM Abs or anti-CD40 Abs for 72 h. Proliferation was assessed by adding [^{3}H]thymidine (1 μCi per well) during the final 16 h of culture, with scintillation counting of harvested cells. Alternatively, B cells were labeled with 2 μM CFSE using a Vybrant CFDA SE Cell Tracer kit (Molecular Probes, Eugene, OR) prior to cell culture. After 72 h, the relative number of viable cells (from 2×10^4 events recorded) and the level of CFSE staining was assessed by FACS. For assessment of lymphoblast development, B cells were cultured (3.75×10^6 in 1.5 ml of medium/well) in 24-well tissue culture plates, followed by treatment with F(ab′)$_2$ anti-IgM and/or anti-CD40 Abs. After 18 or 48 h, the cells were harvested, washed, and resuspended in PBS containing 5 μg/ml propidium iodide (PI) (Sigma-Aldrich, St. Louis, MO). FACS analysis was used to evaluate cell size (forward scatter (FSC)) and viability (PI uptake). For assessment of apoptosis, purified splenic B cells were cultured as above in 24-well tissue culture plates with F(ab′)$_2$ anti-mouse IgM (40 μg/ml) or anti-CD40 (1 μg/ml) Abs. After 18 and 48 h, the cells were harvested and assessed for apoptosis using an Annexin V^{FITC} Apoptosis Detection kit (BD PharMingen) according to the manufacturer's instructions, with 7-aminoactinomycin D (7AAD) (BD PharMingen) substituted for PI to differentiate viable from nonviable cells, followed by FACS analysis.

Immunohistochemistry and TUNEL analysis

Mice were immunized i.p. with 100 μg of 2,4-DNP-keyhole limpet hemocyanin (DNP-KLH; Calbiochem-Novabiochem, La Jolla, CA) in CFA (Sigma-Aldrich). At day 10, the spleens were harvested and frozen in OCT compound (Sakura Finetek, Torrance, CA). Cryostat-cut tissue sections were fixed in acetone for 5 min followed by detection of TUNEL$^+$ cells using a MEBSTAIN apoptosis kit, with detection of biotin-dUTP-incorporated DNA fragments using a streptavidin-alkaline phosphatase secondary reagent (Southern Biotechnology Associates) and a Vector Blue alkaline phosphatase substrate kit (Vector Laboratories, Burlingame, CA). Tissue sections were subsequently counterstained with HRP-conjugated peanut agglutinin (PNA; Sigma-Aldrich) followed by detection using a DAB peroxidase substrate kit (Vector Laboratories). Sections were mounted and visualized using an Olympus IX-70 inverted microscope, with digital images captured using an Optronics MagnaFire digital imaging system.

PI 3-kinase activity

Purified splenic B cells (1.5×10^7 per sample) were resuspended in 0.5 ml of culture medium in sterile 15-ml culture tubes. Following incubation for 5 min at 37°C, the cells were stimulated with F(ab′)$_2$ anti-IgM Abs (40 μg/ml). To stop the reactions, 13 ml of cold Dulbecco's PBS (DPBS) containing 400 μM EDTA and 100 μM Na orthovanadate were added to each tube at the appropriate times. The cells were pelleted and resuspended in lysis buffer containing 1% Nonidet P-40, 150 mM NaCl, 50 mM Tris-HCl (pH 8.0), 1 mM Na orthovanadate, 2 mM EDTA, 50 mM NaF, and 1 mM PMSF. Lysates were precleared using 50 μl of protein G-Sepharose beads (Amersham Pharmacia Biotech, Piscataway, NJ), and then immunoprecipitated with 3 μl of anti-PI 3-kinase Abs for 2 h at 4°C followed by incubation with 50 μl of protein G-Sepharose beads for 2 h at 4°C. The beads were washed twice with lysis buffer, twice in a buffer containing 100 mM Tris-HCl (pH 7.4), 5 mM LiCl, and 100 μM Na orthovanadate, and twice in a buffer containing 10 mM Tris-HCl (pH 7.4), 150 mM NaCl, 5 mM EDTA, and 100 μM Na orthovanadate. The washed beads were then resuspended in 50 μl of the final wash buffer, plus 10 μl of sonicated L-α-phosphatidylinositol (10 mg/ml; Sigma-Aldrich), 10 μl of $MgCl_2$/ATP mixture (Upstate Biotechnology), and 1 μl of [γ-^{32}P]ATP (10 μCi/μl; ICN Biomedicals). The reactions were incubated at 25°C for 15 min before adding 20 μl of 6N HCl and 160 μl of a $CHCl_3$:MeOH (1:1) solution. The samples were then vortexed, and spun for 5 min in a microcentrifuge. Fifteen microliters of the organic (lower) phase of each sample were then spotted onto silica gel thin-layer chromatography plates (Whatman, Clifton, NJ) that were pretreated with a 1% solution of potassium oxalate (Sigma-Aldrich). Plates were developed in a buffer containing 37.5% MeOH, 30% $CHCl_3$, 22.5% pyridine, 1.5% formic acid, 0.04% ethoxyquin, 6% (w/v) boric acid (all from Sigma-Aldrich), and 0.2% (w/v) 2-tert-Butyl-4-methylphenol (Sigma-Aldrich). The plates were analyzed on a PhosphorImager (Molecular Dynamics, Sunnyvale, CA), with relative fluorescence intensities of the regions containing phosphorylated L-α-phosphatidylinositol determined using NIH Image software (version 1.60).

Immunoblotting and intracellular Bad phosphorylation analyses

For immunoblot analyses, purified B cells were cultured in medium as above in sterile culture tubes (2×10^7/ml, 500 μl/tube) or in 24-well tissue culture plates (3.75×10^6 in 1.5 ml medium/well) and treated with F(ab′)$_2$ anti-IgM Abs or anti-CD40 Abs alone or in combination at the indicated concentrations and times. In some experiments, the cells were preincubated for 30 min with 50 nM wortmannin (Sigma-Aldrich) or 15 μM LY294002 (Sigma-Aldrich) prior to stimulation. The reactions were then stopped and the cells lysed as described above. Lysates were subjected to SDS-PAGE followed by electrophoretic transfer to nitrocellulose membranes and subsequent immunoblotting using Abs reactive with phospho-Akt, phospho-Bad, phospho-IκBα, CUL1, ubiquitin, or c-Myc, followed by HRP-conjugated goat anti-rabbit or anti-mouse IgG secondary Abs. Immunoblots were developed using an ECL kit (Pierce, Rockford, IL). To verify equivalent total protein loading, the same blots were stripped and reprobed with Abs reactive with Akt, SHP-1, or ERK2.

For analysis of intracellular Bad phosphorylation, purified splenic B cells were stimulated with F(ab′)$_2$ anti-IgM Abs (40 μg/ml) at 37°C for 5 min, and the reactions stopped as described above. Cells (2.5×10^6/group) were pelleted and fixed in DPBS containing 4% formaldehyde for 20 min, washed in DPBS, and permeabilized in DPBS containing 0.15% Triton

X-100 for 4 min and then blocked for 30 min with DPBS containing 1% FCS, all at room temperature (RT). The cells were incubated 30 min at RT in DPBS containing 1% FCS and a 1/200 dilution of phosphospecific Bad (S136) Abs, washed, and then incubated 30 min with a 1/400 dilution of FITC-conjugated goat anti-rabbit IgG Abs. The cells were spun onto glass slides using a CytoSpin (Shandon, Pittsburgh, PA), with coverslips mounted using Fluoromount-G (Southern Biotechnology Associates). Digital images were obtained using an Olympus IX-70 inverted microscope (Melville, NY) with an IX-FLA fluorescence attachment at ×600 magnification and a 4-s exposure time.

For analysis of $p27^{Kip1}$ and $p21^{Waf1}$ expression, nuclear extracts were prepared from 25×10^6 B6 $CD22^{-/-}$ and wild-type B cells stimulated with $F(ab')_2$ anti-IgM Abs or anti-CD40 Abs for 18 h. Briefly, the cells were lysed at 4°C in a buffer containing 0.4% Nonidet P-40, 10 mM Tris (pH 8.0), 10 mM KCl, 1.5 mM $MgCl_2$, 0.5 mM DTT and protease inhibitors for 20 min with occasional vortexing. The nuclei were pelleted, washed in lysis buffer, and rapidly resuspended in one cell pellet volume of low salt buffer (20 mM Tris (pH 8.0), 25% glycerol, 1.5 mM $MgCl_2$, 0.2 mM EDTA, 20 mM KCl, 0.5 mM DTT, and protease inhibitors), followed by two pellet volumes of high salt buffer (low salt buffer containing 0.6 M KCl), with frequent vortexing over a 20-min period. The extracts were then analyzed for relative protein concentration using a Bio-Rad protein assay kit (Hercules, CA) and by Coomassie Brilliant Blue staining of SDS-PAGE-separated nuclear proteins. Immunobloting analyses were then performed on equivalent total concentrations of nuclear proteins after separation by SDS-PAGE and transfer to nitrocellulose.

cDNA gene arrays

Purified splenic B cells (3.75×10^6 in 1.5 ml medium/well) were cultured in 24-well tissue culture plates at 37°C with 5% CO_2. The cells were stimulated with $F(ab')_2$ anti-IgM or anti-CD40 Abs for 18 h as described above. Total RNA from 1×10^7 B cells was isolated from harvested cells using a RNeasy kit (Qiagen, Valencia, CA). RNA (2.5 μg) was then subjected to cDNA synthesis and gene array hybridization using GEArray Q Series mouse radioactive cDNA expression array kits specific for genes in the cell cycle pathway (SuperArray, Bethesda, MD) according to the manufacturer's instructions. Reagents used for cDNA synthesis not provided in the kits included [α-^{32}P]dCTP (ICN Biomedicals) and SuperScript II reverse transcriptase (Invitrogen, Carlsbad, CA). Radioactivity on the arrays was detected using a phosphorimager.

Statistical analysis

All data are shown as mean values ± SEM unless stated otherwise. The Student *t* test was used to determine the level of significance in differences between sample means.

Results

Highly impaired IgM-induced proliferation of B6 $CD22^{-/-}$ B cells

B cells from founder B6/129 $CD22^{-/-}$ mice generated in our laboratory exhibited significant, but moderate, reductions in their ability to proliferate in response to IgM ligation (10–70% decrease, Fig. 1), as previously described (19). However, when the CD22 deficiency was backcrossed onto a B6 genetic background for eight generations, the defect in IgM-induced proliferation became severe over a range of anti-IgM Ab concentrations (90–99% decrease, Fig. 1). The failure of B6 $CD22^{-/-}$ B cells to respond to anti-IgM Abs did not result from a general inability to proliferate, as both B6 $CD22^{-/-}$ and B6/129 $CD22^{-/-}$ B cells were hyperresponsive to CD40-induced proliferation compared to B cells from their wild-type littermates (100–400% increase, Fig. 1). Thus, $CD22^{-/-}$ B cell proliferation following IgM engagement was more highly impaired in the context of a B6 genetic background, while augmented CD40-induced proliferation was not influenced by genetic background.

Consistent with the failure of B6 $CD22^{-/-}$ B cells to incorporate [^{3}H]thymidine, analysis of clonal expansion by CFSE-labeling revealed that B6 $CD22^{-/-}$ B cells failed to undergo significant rounds of clonal expansion following IgM ligation (Fig. 2*A*). By contrast, B cells from wild-type littermates underwent multiple rounds of proliferation. Also consistent with [^{3}H]thymidine incorporation, clonal expansion of B6 $CD22^{-/-}$ B cells was augmented in response to CD40 ligation alone. However, IgM plus CD40 ligation induced high-level clonal expansion in both $CD22^{-/-}$ and wild-type B cell cultures. Thus, B6 $CD22^{-/-}$ B cells did not clonally expand unless survival or costimulatory signals were provided through a CD40-dependent signaling pathway.

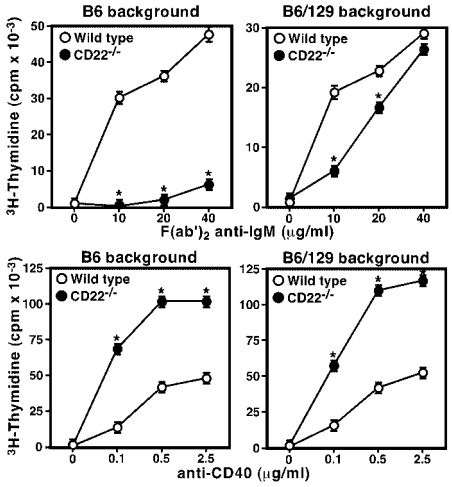

FIGURE 1. Comparison of proliferative responses of B6 $CD22^{-/-}$ and B6/129 $CD22^{-/-}$ B cells following IgM and CD40 ligation. Purified splenic B cells from B6 $CD22^{-/-}$, B6/129 $CD22^{-/-}$, or wild-type littermate mice were stimulated with the indicated concentrations of $F(ab')_2$ anti-IgM or anti-CD40 Abs during 72-h proliferation assays. Values represent the mean (±SEM) cpm of [^{3}H]thymidine uptake in triplicate cultures. Results represent one of three independent experiments producing similar results. *, Significant differences between sample means, $p < 0.01$.

B cells from B6 $CD22^{-/-}$ mice did not develop into large lymphoblasts following IgM ligation (Fig. 2*B*). The progression of small, resting B cells into lymphoblasts was assessed based on increased FSC as a measure of cell size, with cell death visualized by PI uptake. Compared with wild-type B cells, there was a dramatic reduction of lymphoblasts in $CD22^{-/-}$ B cell cultures after IgM ligation (8 ± 1% $CD22^{-/-}$ vs 34 ± 3% wild-type; $p < 0.01$, $n = 4$, Fig. 2*B*). Importantly, early lymphoblast formation after IgM ligation (18 h) was similar between B6 $CD22^{-/-}$ and wild-type B cell cultures, but the frequency of lymphoblasts in $CD22^{-/-}$ cultures did not increase further after 48 h of stimulation (Fig. 2*C*). Moreover, lymphoblast generation was broadly deficient in $CD22^{-/-}$ B cell cultures stimulated with graded concentrations of $F(ab')_2$ anti-IgM Abs, while wild-type B cells responded to anti-IgM Ab concentrations of 15–40 μg/ml (Fig. 2*D*). By contrast, CD40 ligation or IgM plus CD40 ligation resulted in lymphoblast generation in both $CD22^{-/-}$ and wild-type cultures (Fig. 2*B*). As such, B6 $CD22^{-/-}$ B cells may be predisposed to undergo apoptosis following IgM engagement unless costimulatory signals are provided by CD40 ligation.

Augmented IgM-induced apoptosis of B6 $CD22^{-/-}$ B cells

To determine whether impaired IgM-induced proliferation and lymphoblast development in B6 $CD22^{-/-}$ B cell cultures correlated with augmented programmed cell death, the rate of IgM-induced apoptosis in B6 $CD22^{-/-}$ B cell cultures was assessed. Annexin V and 7AAD staining of cultured B cells followed by FACS analysis was used to differentiate between annexin V^+/$7AAD^+$ (apoptotic, nonviable), annexin V^+/$7AAD^-$ (apoptotic, viable) and annexin V^-/$7AAD^+$ (necrotic) cells. After 18 h of culture, the percentages of B cells present within gated regions representing the above populations was similar between B6

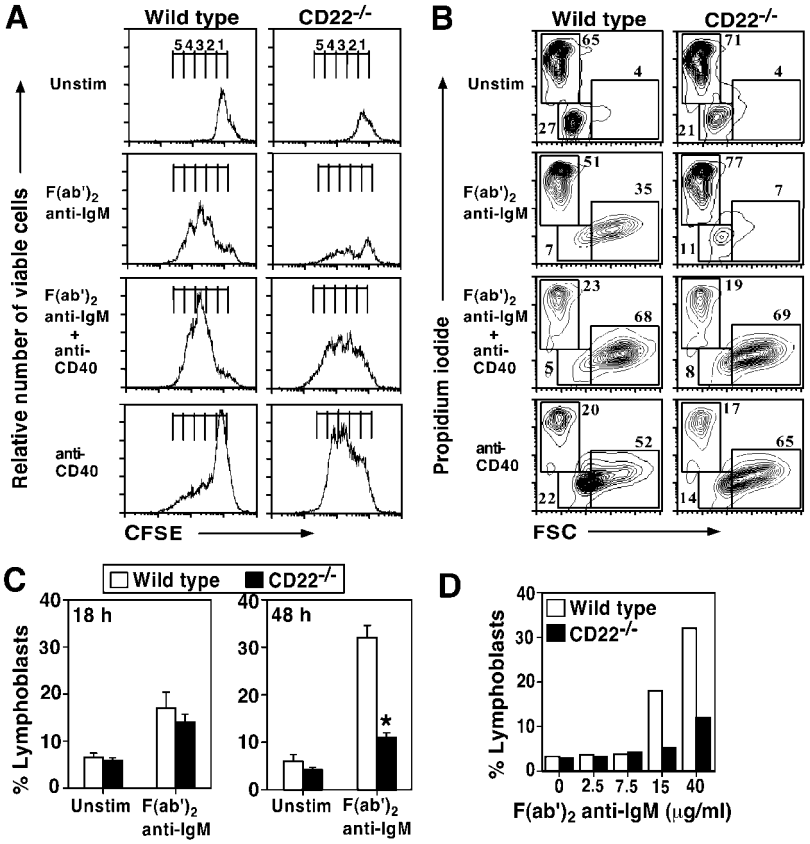

FIGURE 2. Impaired clonal expansion and lymphoblast development of B6 CD22$^{-/-}$ B cells following IgM ligation, and rescue by CD40 ligation. *A*, Purified splenic B cells from B6 CD22$^{-/-}$ and wild-type mice were labeled with CFSE and then cultured with F(ab′)$_2$ anti-IgM (40 μg/ml) Abs and/or anti-CD40 (1 μg/ml) Abs. After 72 h, the cells were stained with PI and analyzed for CFSE fluorescence. A constant number of cells (2×10^4) were assessed for each histogram, with viable (PI$^-$) cells shown. Sequential peaks of decreased CFSE fluorescence intensity identify subsequent generations of proliferating daughter cells. The parental cell generation (1) and subsequent proliferating daughter cell generations (2–5) are as indicated. Results represent one of three independent experiments producing similar results. *B*, Purified splenic B cells from B6 CD22$^{-/-}$ and wild-type mice were cultured with F(ab′)$_2$ anti-IgM (40 μg/ml) Abs and/or anti-CD40 (1 μg/ml) Abs. After 48 h, the cells were harvested and immediately analyzed for viability (PI exclusion) and cell size (FSC). Numbers represent the percentage of cells within the indicated gates. Results represent one of four experiments producing similar results. *C*, Values represent the mean (±SEM) percentages of lymphoblasts from four independent experiments as shown in *B*, cultured for 18 or 48 h. ∗, Significant differences between sample means, $p < 0.01$. *D*, Effect of decreased valency of IgM ligation on B6 CD22$^{-/-}$ B lymphoblast development. Purified splenic B cells were cultured with the indicated concentrations of F(ab′)$_2$ anti-IgM Abs for 48 h and analyzed as described in *B*. Results represent one of two independent experiments producing similar results.

CD22$^{-/-}$ and wild-type B cell cultures (Fig. 3*A*). However, after 48 h of culture, there was a dramatic increase in the frequency of annexin V$^+$/7AAD$^+$ (apoptotic, nonviable) B cells in anti-IgM-stimulated CD22$^{-/-}$ B cell cultures compared to wild-type cultures. The percentage of annexin V$^+$/7AAD$^-$ (apoptotic, viable) cells was similar between genotypes at this time point, suggesting that the transition time from this stage to the annexin V$^+$/7AAD$^+$ stage is rapid in primary B cells. By contrast, CD22$^{-/-}$ or wild-type B cells treated with anti-CD40 Abs were mostly rescued from apoptosis (Fig. 3*A*). Thus, B6 CD22$^{-/-}$ B cells were either induced to undergo apoptosis or did not receive appropriate survival signals following IgM ligation.

Spleen B cells in the CD22$^{-/-}$ mice used for these studies had a high spontaneous turnover rate in vivo (data not shown), as described previously for other lines of CD22$^{-/-}$ mice (16, 18). However, that CD40 ligation rescued B6 CD22$^{-/-}$ B cells from apoptosis in vitro (Fig. 3*A*) suggested that germinal center development may proceed normally in B6 CD22$^{-/-}$ mice immunized with a T cell-dependent Ag. Therefore, the location of apoptotic cells in the spleens of B6 CD22$^{-/-}$ mice was analyzed during an immune response to the T-dependent Ag, DNP-KLH. Spleen lymphoid follicles in B6 CD22$^{-/-}$ mice contained a markedly higher level of TUNEL$^+$ cells compared to follicles in wild-type littermate mice (Fig. 3*B*), including a prominent ring of apoptotic cells at the follicle periphery that likely represents the marginal zone (MZ), a region that is reduced in CD22$^{-/-}$ mice (29). Despite this, overall follicle size and frequency was similar between CD22$^{-/-}$ and wild-type littermates, and there were no obvious differences in germinal center size or in the frequency of TUNEL$^+$ cells within germinal centers (Fig. 3*B* and data not shown). In addition, although the frequency of germinal centers was significantly reduced in naive B6 CD22$^{-/-}$ mice, germinal center frequency was augmented following immunization to levels equivalent to that of wild-type mice (Fig. 3*C*). Therefore, although the frequency of apoptotic cells was augmented in lymphoid follicles of B6 CD22$^{-/-}$ mice, germinal center development was not impaired.

B6 CD22$^{-/-}$ B cells have a complex cell surface phenotype

IgM-induced apoptosis is a hallmark of both immature B cells and peritoneal B-1 (CD5$^+$) B cells (30–33). CD5 expression by anergic B cells correlates with their lack of IgM-induced proliferation (34), while a loss of CD5 expression restores IgM-induced proliferation in both B-1 and anergic B cells (30, 34). Therefore, the cell surface phenotype of splenic B6 CD22$^{-/-}$ B cells was assessed to determine whether they share phenotypic properties with immature or anergic B cells. Uniquely, splenic B cells from B6 CD22$^{-/-}$ mice expressed uniformly high levels of HSA, decreased levels of IgD and CD21, and were predominantly CD5$^+$, in contrast with the majority of splenic B cells from B6/129 CD22$^{-/-}$ mice and wild-type littermate mice of each genetic background (Fig. 4*A*). The intermediate level of CD5 expressed on splenic B6 CD22$^{-/-}$ B cells was distinct from the higher levels of CD5 expressed by small numbers of B-1 B cells present in all mouse genotypes (data not shown). Moreover, the intermediate level of CD5 expressed on splenic B6 CD22$^{-/-}$ B cells correlated closely with levels previously found on anergic B cells (34). Nevertheless, B cells from both B6 and B6/129 CD22$^{-/-}$ mice exhibited decreased IgM and increased MHC class II levels, as previously reported (16, 18, 19).

Because B6 CD22$^{-/-}$ B cells exhibited augmented HSA expression, a detailed analysis of mature and transitional B cell populations was performed, as described previously (35). There were similar percentages of CD23$^+$/IgD$^+$/IgM^{low} (mature), CD23$^+$/IgD$^+$/IgM^{high} (transitional type 2, T2) and CD23$^-$/IgD$^-$/IgM^{high} (transitional type 1, T1, + MZ) B cells in the spleens of B6 CD22$^{-/-}$ and wild-type mice (Fig. 4*B*). An additional analysis of

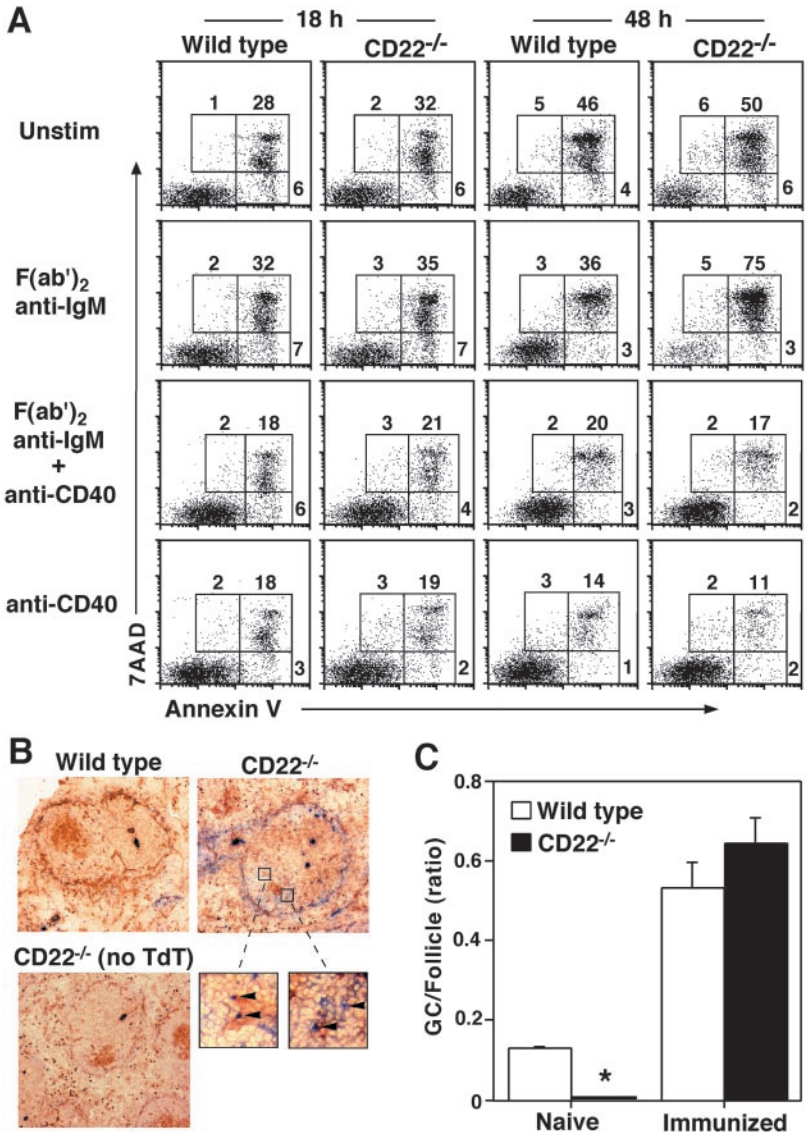

FIGURE 3. Augmented apoptosis of B6 CD22$^{-/-}$ B cells. *A*, CD22$^{-/-}$ B cell apoptosis in vitro. Purified splenic B cells from B6 CD22$^{-/-}$ and wild-type littermate mice were cultured with F(ab′)$_2$ anti-IgM Abs (40 μg/ml) or anti-CD40 Abs (1 μg/ml). After 18 and 48 h, the cells were harvested and apoptotic cells were identified by annexin V and 7AAD staining followed by FACS analysis. *B*, Apoptosis within lymphoid follicles of CD22$^{-/-}$ mice. B6 CD22$^{-/-}$ and wild-type littermate mice were immunized i.p. with DNP-KLH. Ten days later, apoptotic cell death was identified by TUNEL staining of spleen sections, with apoptotic cells indicated by blue color. Spleen sections were counterstained with PNA (brown color) to identify secondary follicles. Enlarged regions indicated by squares show the presence of pyknotic nuclei (arrowheads). As a control for TUNEL staining, a CD22$^{-/-}$ spleen section was subjected to the TUNEL procedure without TdT added, followed by PNA staining. Results represent spleen sections from three mice of each genotype producing similar results. *C*, Germinal center (GC)-to-follicle ratios in naive B6 CD22$^{-/-}$ and wild-type mice and mice immunized with DNP-KLH as in *B*. Values represent mean (±SEM) GC-to-follicle ratio in three to four mice of each genotype. *, Significant differences between sample means, $p < 0.05$.

T1 cells, CD21^{-}/IgD^{-}/IgM^{high}, confirmed a similar percentage of this population between B6 CD22$^{-/-}$ and wild-type mice (data not shown). Thus, B6 CD22$^{-/-}$ B cells uniquely expressed cell surface markers associated with anergic/chronically stimulated B cells, without any disruption in the percentages of mature and transitional B cell populations.

Decreased numbers of circulating B cells is another hallmark of CD22$^{-/-}$ mice, although spleen B cell numbers are normal (16, 18, 19). This reduction was shared by B6 CD22$^{-/-}$ and B6/129 CD22$^{-/-}$ mice, relative to their wild-type littermates, although the difference was more pronounced on the B6 genetic background (Fig. 4*C*). Nevertheless, numbers of spleen B220^{+} B cells were similar between both B6 CD22$^{-/-}$ and B6/129 CD22$^{-/-}$ mice and their wild-type littermates (Fig. 4*C*).

Intact PI 3-kinase and Akt activation in B6 CD22$^{-/-}$ B cells

PI 3-kinase activity is required for B cells to develop into large lymphoblasts and proliferate following IgM ligation (36, 37), and tyrosine-phosphorylated CD22 recruits PI 3-kinase (25, 38). Therefore, we assessed whether impaired PI 3-kinase activity in B6 CD22$^{-/-}$ B cells was a potential cause for their failure to undergo IgM-induced proliferation. PI 3-kinase activity during in vitro kinase assays was similar between resting B cells from CD22$^{-/-}$ and wild-type littermates, and increased at similar levels following IgM ligation (Fig. 5*A*), indicating that PI 3-kinase activity was intact in B6 CD22$^{-/-}$ B cells.

A major downstream target of PI 3-kinase is the serine/threonine kinase Akt, which promotes cell survival (39, 40) and is activated following IgM ligation (41). PI 3-kinase-dependent phosphorylation of Akt on the regulatory amino acids threonine 308 (T308) and serine 473 (S473) results in its full activation (42). Surprisingly, Akt phosphorylation at T308 and S473 was constitutively higher in B6 CD22$^{-/-}$ B cells compared to wild-type B cells, as well as following IgM ligation (Fig. 5*B*).

Akt activation leads to phosphorylation of the Bcl-2 family member Bad, and the cytoplasmic inhibitor of NF-κB, IκBα. Phosphorylation of Bad by Akt at either serine 136 (S136) or serine 112 (S112) promotes cell survival by reducing its inhibition of the antiapoptotic proteins Bcl-x$_L$ and Bcl-2 (43–45). As was observed for Akt activity, Bad was phosphorylated at higher levels in B6 CD22$^{-/-}$ B cells on both S112 and S136 compared to wild-type cells prior to and following IgM ligation (Fig. 5*B*). Intracellular staining of resting and activated B cells with phosphospecific S136 Abs also revealed a greater staining intensity of Bad by the majority of B6 CD22$^{-/-}$ B cells (Fig. 5*C*), suggesting that Bad hyperphosphorylation was not restricted to a subset of CD22$^{-/-}$ B

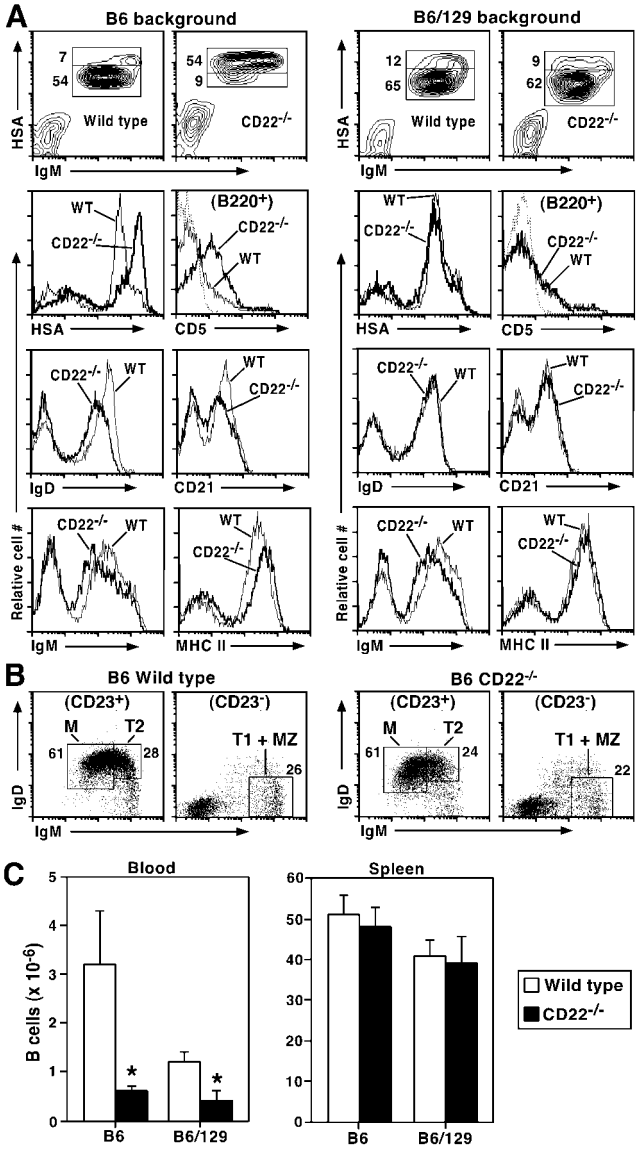

FIGURE 4. B6 CD22$^{-/-}$ B cells have a unique phenotype. *A*, Cell surface protein expression levels on splenocytes from B6 CD22$^{-/-}$ mice, B6/129 CD22$^{-/-}$ mice, and their wild-type littermates. Numbers (*top panels*) represent the percentage of HSA^{high} or HSA^{low} cells within the indicated gates. *B*, Mature and transitional B cell populations in B6 CD22$^{-/-}$ and wild-type mice. Splenocytes were stained with Abs reactive with CD23, IgD, and IgM. Numbers represent the percentage of cells within the indicated gates for either the CD23^{+} or CD23^{-} populations. M, mature; T2, transitional type 2; T1, transitional type 1. Results in *A* and *B* are representative of similar results obtained from three mice of each genotype. *C*, Numbers of blood and spleen B cells in B6 CD22$^{-/-}$ mice, B6/129 CD22$^{-/-}$ mice, and their wild-type littermates. Values for blood represent B cells per milliliter. Values represent mean (±SEM) cell numbers from four mice of each genotype. ∗, Significant differences between sample means, $p < 0.01$.

cells. Thus, IgM-induced Akt phosphorylation and activity were not impaired in CD22$^{-/-}$ B cells.

The transcription factor NF-κB is activated following IgM ligation (46), and NF-κB transcriptional activity has been linked with protection of cells from apoptotic stimuli (47, 48). Active Akt phosphorylates and activates IκB-kinase α (49), a component of a kinase complex that in turn phosphorylates IκBα at serine 32 (S32) and serine 36 (S36). These phosphorylation events initiate IκBα ubiquitination and degradation, resulting in the release of active NF-κB. In B6 CD22$^{-/-}$ B cells, IκBα was phosphorylated at higher levels before and following IgM ligation compared to wild-type cells (Fig. 5*D*). Enhanced IgM-induced Akt, IκBα, and Bad phosphorylation in B6 CD22$^{-/-}$ B cells was a PI 3-kinase-dependent process, as confirmed by pretreatment with wortmannin or LY294002, which reduced Akt, IκBα, and Bad phosphorylation to levels found in unstimulated B cells (Fig. 5*E*). Collectively, these results suggest that CD22 expression normally suppresses Akt activation and phosphorylation of its downstream targets. Also, as CD22 deficiency did not disrupt activation of the PI 3-kinase/Akt pathway, it is likely that the inability of B6 CD22$^{-/-}$ B cells to develop into lymphoblasts and proliferate results from alterations in survival or proliferation signals that are further downstream during IgM signal transduction.

Impaired induction of c-Myc and CUL1 ubiquitin ligase complex protein in B6 CD22$^{-/-}$ B cells

Because the percentage of B cells that developed into early lymphoblasts was similar between B6 CD22$^{-/-}$ and wild-type B cell cultures (18 h after IgM ligation, Fig. 2*C*), the high level of cell death observed in 48-h cultures was likely to reflect incomplete cell cycle progression, rather than early IgM signaling defects. To identify such defects in B6 CD22$^{-/-}$ B cells, cDNA arrays for cell cycle-regulated genes were used. In these assays, B cells were cultured with F(ab′)$_2$ anti-IgM Abs for 18 h to ensure that both CD22$^{-/-}$ and wild-type B cells were at similar levels of viability when cellular RNA was isolated. Of the cell cycle regulatory genes observed to be expressed following IgM ligation, there was a severe deficit in transcripts for the ubiquitin ligase complex protein CUL1 in B6 CD22$^{-/-}$ B cells (Fig. 6*A*). Likewise, IgM ligation did not induce CUL1 protein expression above basal levels in B6 CD22$^{-/-}$ B cells, while CUL1 protein was induced in wild-type B cells (Fig. 6*B*). The lack of augmented CUL1 expression in B6 CD22$^{-/-}$ B cells following IgM ligation also correlated with impaired ubiquitination of cellular proteins, especially in the range of ~28–50 kDa (Fig. 6*B*). However, CD40 coligation or ligation alone completely restored CUL1 expression and total protein ubiquitination to wild-type levels in B6 CD22$^{-/-}$ B cells (Fig. 6*B*). Gene array analysis also confirmed normal CUL1 transcript expression following CD40 ligation in B6 CD22$^{-/-}$ B cells (data not shown). Thus, IgM-ligation failed to induce CUL1 transcripts or protein in B6 CD22$^{-/-}$ B cells, while CD40 ligation induced CUL1 expression.

CUL1 expression relies on c-Myc transcriptional activity (27). Therefore, c-Myc expression was examined in CD22$^{-/-}$ B cells following IgM ligation. Strikingly, c-Myc was expressed more transiently and at much lower levels in B6 CD22$^{-/-}$ B cells following IgM ligation compared with wild-type B cells, with undetectable increases above baseline at 18 h (Fig. 6*C*). c-Myc expression in a whole cell lysate of purified B cells from a mouse that constitutively overexpresses c-Myc protein (50) is shown as a positive control. In addition, CD40 coligation or ligation alone induced c-Myc protein expression at similar, high levels in both B6 CD22$^{-/-}$ and wild-type B cells after 18 h of stimulation (Fig. 6*D*). Both CUL1 and c-Myc were expressed in B6/129 CD22$^{-/-}$ B cells at levels similar to wild-type B cells following IgM ligation alone (Fig. 6, *E* and *F*), which correlated with their near-normal proliferation (Fig. 1). Therefore, impaired c-Myc induction following IgM ligation in B6 CD22$^{-/-}$ B cells directly correlates with defective CUL1 expression and protein ubiquitination.

Cell cycle inhibitory proteins such as the cyclin-dependent kinase inhibitors p27^{Kip1} and p21^{Waf1} are targeted for ubiquitination and subsequent degradation as a result of CUL1 expression in other cell systems (27, 51, 52). Therefore, we examined whether

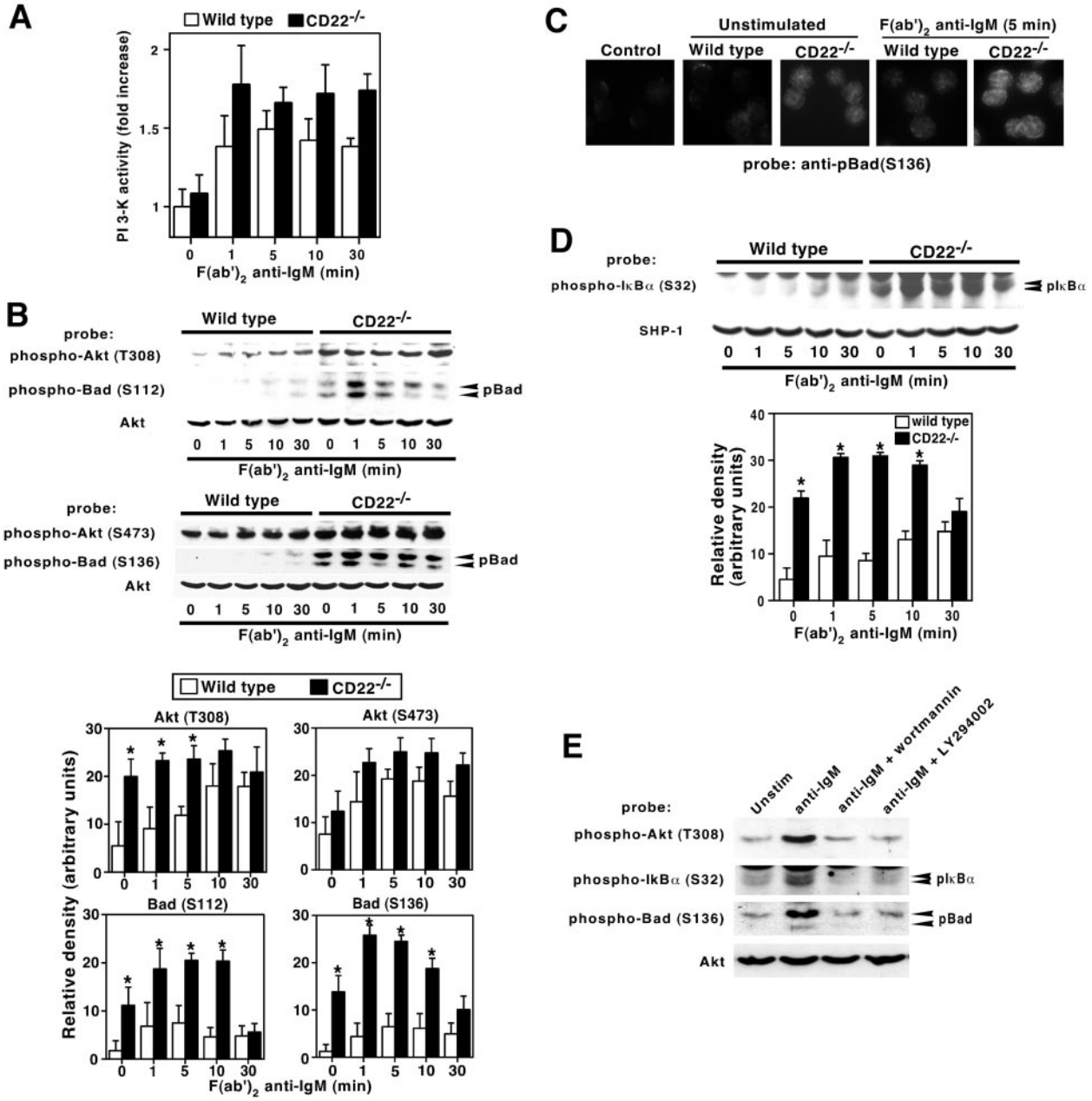

FIGURE 5. PI 3-kinase and Akt activity in B6 CD22$^{-/-}$ B cells. *A*, Purified B6 CD22$^{-/-}$ or wild-type splenic B cells were stimulated with F(ab′)$_2$ anti-IgM Abs (40 μg/ml) for the times indicated, detergent lysed, and immunoprecipitated with anti-PI 3-kinase Abs. PI 3-kinase activity was examined in vitro in the presence of L-α-phosphatidylinositol and [γ-^{32}P]ATP, with phospholipids separated by TLC followed by analysis of regions containing 3′-phosphorylated phosphatidylinositol. Values represent mean (±SEM) relative phosphatidylinositol phosphorylation levels from three independent experiments. PI 3-kinase activation levels for untreated wild-type B cells (time 0) were adjusted to 1.0, with all other values shown relative to this. *B*, Purified B6 CD22$^{-/-}$ or wild-type splenic B cells were stimulated with F(ab′)$_2$ anti-IgM Abs (40 μg/ml) for the times indicated and detergent lysed. Cellular proteins were separated by SDS-PAGE, transferred to nitrocellulose membranes, and immunoblotted using Abs reactive with phosphorylated Akt or Bad. To verify equal amounts of protein in each lane, the same blots were stripped and reprobed with anti-Akt Abs. Bar graphs indicate relative band intensities from four independent immunoblotting experiments. Values represent mean (±SEM) optical densities. ∗, Significant differences between mean values, $p < 0.01$. *C*, Immunofluorescence analysis of Bad phosphorylation. Purified B6 CD22$^{-/-}$ or wild-type splenic B cells were stimulated with F(ab′)$_2$ anti-IgM Abs (40 μg/ml), fixed onto glass slides, permeabilized, and stained with anti-phospho-Bad (S136) Abs. *D*, IκBα phosphorylation. B6 CD22$^{-/-}$ or wild-type splenic B cells were stimulated as in *B*, with immunoblot analyses performed using Abs specific for IκBα phosphorylated at S32. Membranes were then stripped and reprobed with anti-SHP-1 Abs. Relative band intensities of phosphorylated IκBα were determined, and values represent mean (±SEM) optical densities from four experiments. ∗, Significant differences between mean values, $p < 0.01$. *E*, PI 3-kinase inhibitors reduce IgM-mediated Akt, Bad, and IκBα phosphorylation in B6 CD22$^{-/-}$ B cells. Splenic B6 CD22$^{-/-}$ B cells were cultured untreated or were preincubated for 30 min with wortmannin or LY294002 and then stimulated with F(ab′)$_2$ anti-IgM Abs (40 μg/ml) for 5 min. Immunoblot analysis was then performed on cell lysates using Abs specific for phosphorylated Akt (T308), IκBα (S32), or Bad (S136). The Akt portion of the blot was reprobed with anti-Akt Abs to verify equivalent protein loading.

defective CUL1 induction in IgM-stimulated B6 CD22$^{-/-}$ B cells correlated with impaired degradation of p27^{Kip1} or p21^{Waf1}. Remarkably, protein levels of both p27^{Kip1} and p21^{Waf1} were reduced in wild-type B cells following IgM ligation alone, while their reduction in B6 CD22$^{-/-}$ B cells was impaired (Fig. 6*G*). However, CD40 costimulation reduced p27^{Kip1} expression modestly and

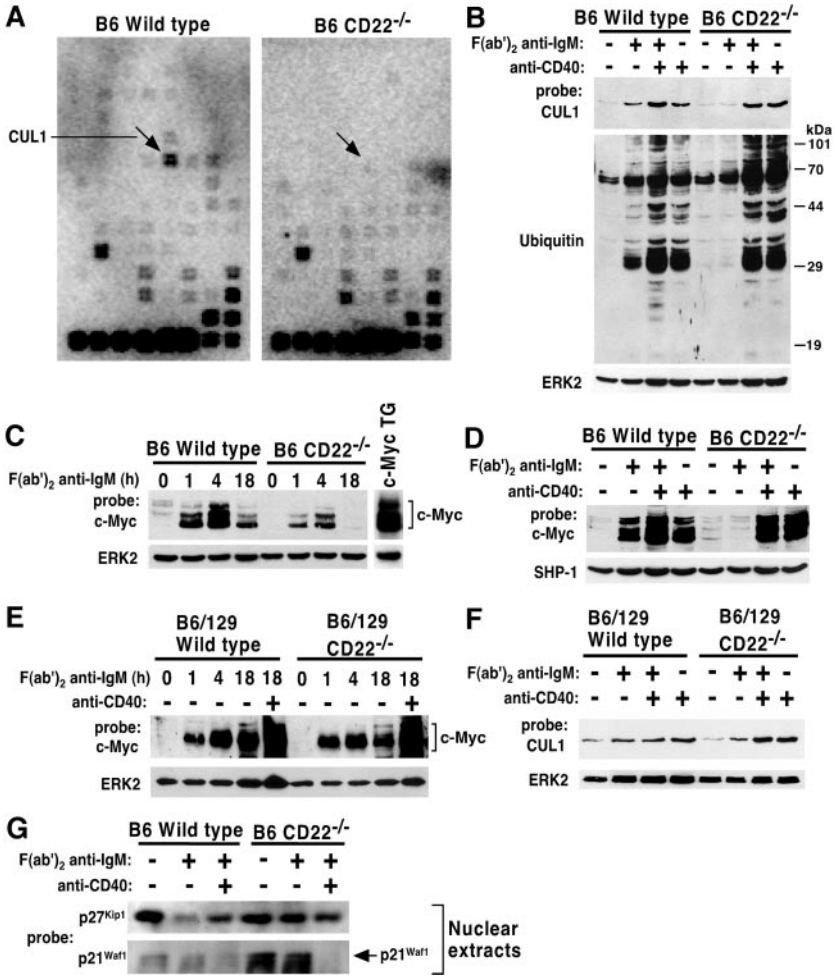

FIGURE 6. Defective induction of the c-Myc:CUL1 ubiquitin ligase pathway in B6 CD22$^{-/-}$ B cells. *A*, cDNA gene array analysis of cell cycle genes was performed on total RNA from B6 CD22$^{-/-}$ or wild-type B cells stimulated for 18 h with F(ab′)$_2$ anti-IgM Abs (40 μg/ml). Arrows show the position of the CUL1 gene on the arrays. *B*, Impaired CUL1 expression and protein ubiquitination in IgM-stimulated B6 CD22$^{-/-}$ B cells. B6 CD22$^{-/-}$ or wild-type B cells were stimulated for 18 h with F(ab′)$_2$ anti-IgM Abs (40 μg/ml) alone or in combination with anti-CD40 Abs (1 μg/ml), or with anti-CD40 Abs alone (1 μg/ml). Total cellular proteins were separated by SDS-PAGE, followed by immunoblot analyses for CUL1 expression, and total protein ubiquitination. Membrane reprobes with Abs specific for ERK2 expression were performed as controls for protein loading. *C* and *D*, Impaired c-Myc induction in IgM-stimulated B6 CD22$^{-/-}$ B cells. *C*, B6 CD22$^{-/-}$ and wild-type B cells were stimulated with F(ab′)$_2$ anti-IgM Abs (40 μg/ml) for the time periods indicated, and cellular proteins subjected to immunoblot analyses for the induction of c-Myc expression. Membrane reprobes with Abs against ERK2 were performed as a control for protein loading. c-Myc expression in a whole cell lysate of purified B cells from a c-Myc transgenic (c-Myc TG) mouse (50) is shown as a positive control. *D*, B6 CD22$^{-/-}$ and wild-type B cells were treated as in *B* for 18 h and cellular proteins subjected to SDS-PAGE and immunoblot analyses for the induction of c-Myc expression. Membrane reprobes with Abs against SHP-1 were performed as controls for protein loading. *E* and *F*, c-Myc and CUL1 expression is not impaired in B6/129 CD22$^{-/-}$ B cells. B6/129 CD22$^{-/-}$ and wild-type B cells were stimulated with F(ab′)$_2$ anti-IgM Abs (40 μg/ml) or anti-CD40 Abs (1 μg/ml) as above, and cellular proteins were subjected to immunoblot analyses for the induction of c-Myc (*E*) and CUL1 (*F*) expression. Results in *B–F* represent one of three independent experiments producing similar results. *G*, Impaired degradation of cell cycle inhibitor proteins in IgM-stimulated B6 CD22$^{-/-}$ B cells. B6 CD22$^{-/-}$ and wild-type B cells were stimulated for 18 h with F(ab′)$_2$ Abs or anti-CD40 Abs as described above. Equivalent total protein concentrations of nuclear extracts were separated by SDS-PAGE, followed by immunoblotting analyses for p27^{Kip1} and p21^{Waf1} expression. Results represent one of two independent experiments producing similar results.

p21^{Waf1} expression to nearly undetectable levels in B6 CD22$^{-/-}$ B cells, correlating with the ability of CD40 to rescue their proliferative capacity (Figs. 1 and 2).

Discussion

The current study defines CD22 as a critical regulator of B cell proliferation, survival, phenotype, and the expression of essential cell cycle regulatory genes, especially in the context of a B6 genetic background. B6 CD22$^{-/-}$ B cells were highly refractory to IgM-induced proliferation as indicated by their inability to generate lymphoblasts (Fig. 2, *B–D*) and clonally expand (Figs. 1 and 2*A*). CD22 deficiency also resulted in enhanced B cell apoptosis in vitro and in vivo (Fig. 3). The proliferative defect and augmented apoptosis of B6 CD22$^{-/-}$ B cells did not result from the failure of IgM to generate positive transmembrane signals (Fig. 5). Likewise, B6 CD22$^{-/-}$ B cells were not absolutely programmed to undergo apoptosis following activation, as CD40 engagement induced augmented proliferation and clonal expansion of both B6 CD22$^{-/-}$ and B6/129 CD22$^{-/-}$ B cells (Figs. 1 and 2). Also, germinal center formation was normal in B6 CD22$^{-/-}$ mice following Ag challenge (Fig. 3, *B* and *C*). Rather, the proliferative defect and augmented apoptosis of B6 CD22$^{-/-}$ B cells following IgM ligation correlated with their unique cell surface phenotype (Fig. 4*A*) and defective induction of the c-Myc:CUL1 ubiquitin ligase pathway (Fig. 6). These findings support the previous concept by us and others that CD22 expression influences multiple B cell signaling

pathways, likely through the regulation of both negative and positive effector molecules (8, 15, 25, 26, 38, 53).

B cells from B6 CD22$^{-/-}$ mice uniquely expressed high levels of HSA along with low IgD and CD21 levels (Fig. 4*A*), all characteristics of immature/transitional B cells (54). It is well-established that BCR engagement on immature B cells results in death by apoptosis (31). The prevalence of B cells with an immature/transitional phenotype in B6 CD22$^{-/-}$ mice could result as a consequence of rapid B cell turnover, as indicated by their increased rate of apoptosis in vivo (Fig. 3*B*). However, B6/129 CD22$^{-/-}$ B cells also had high turnover rate in vivo (data not shown), as in another line of B6/129 CD22$^{-/-}$ mice (18), yet did not share these phenotypic characteristics of B6 CD22$^{-/-}$ B cells (Fig. 4*A*). In addition, a detailed analysis of B cell subsets in B6 CD22$^{-/-}$ mice revealed similar percentages of mature, T2, and T1 B cells to those found in wild-type mice (Fig. 4*B*), indicating that the distribution of these subsets is not perturbed. B6 CD22$^{-/-}$ B cells also uniquely expressed intermediate levels of CD5 (Fig. 4*A*), indicative of chronically activated and/or tolerized B cells (34). A similar shift to a CD5^{+} B-1-like phenotype is found in B cells expressing an Ig transgene specific for Sm, an autoantigen frequently involved in systemic lupus erythematosus (55). B6 CD22$^{-/-}$ B cells also demonstrated an IgM^{low}/MHC class II^{high} phenotype that is found on self-reactive/tolerized B cells (56). The IgM^{low}/MHC class II^{high} phenotype is also shared by mice that overexpress CD19 (57), as well as B cells from B6/129 CD22$^{-/-}$ mice used in this study (Fig. 4*A*) and other lines of CD22$^{-/-}$ mice (16–18). Thus, CD22 deficiency in the context of a B6 genetic background results in B cells with a unique, chronically stimulated phenotype that results in the inability of these cells to respond to IgM-induced proliferation.

The proliferative defect and augmented apoptosis of B6 CD22$^{-/-}$ B cells did not result from the inability of cell surface IgM to generate transmembrane signals. In fact, B cells from the B6 CD22$^{-/-}$ mice used in these studies exhibit normal ERK activation (15), CD19 phosphorylation (data not shown), and PI 3-kinase activity (Fig. 5*A*). In addition, the activation of Akt, which is downstream of PI 3-kinase signaling, was augmented in B6 CD22$^{-/-}$ B cells, both basally and following IgM ligation (Fig. 5*B*). Importantly, enhanced Akt activation correlated with Bad and IκBα hyperphosphorylation (Fig. 5, *B–D*), two events that normally correlate with augmented cell survival (43–45, 47–49). Thus, defective proliferation and survival of B6 CD22$^{-/-}$ B cells may result from impaired signaling events that are independent of these signaling pathways. Alternatively, heightened baseline and IgM-induced activation of Akt in B6 CD22$^{-/-}$ B cells may alter the kinetics and/or intensity of downstream signaling events critical to sustaining lymphoblast development and promoting cell cycle progression. In support of this, we have previously shown that B cells from this line of B6 CD22$^{-/-}$ mice are defective in c-jun N-terminal kinase (JNK) activation following IgM ligation (15), an event that has been suggested by others to possibly reflect a desensitization mechanism resulting from moderately augmented basal JNK activation levels (53). Likewise, IgM ligation does not induce JNK activation in chronically activated (self-reactive/tolerant) B cells in the anti-hen egg lysozyme transgenic mouse model of B cell tolerance (46). Thus, CD22 deficiency on a B6 genetic background may alter the proliferative potential of B cells through pathways that are also exercised by self-reactive B cells.

That B6 CD22$^{-/-}$ B cells failed to clonally expand and predominantly underwent IgM-induced death suggested impaired cell cycle progression, consistent with the observation that early survival and lymphoblast development (18 h following IgM ligation) were not impaired in B6 CD22$^{-/-}$ B cell cultures (Fig. 2*C* and data not shown). Supporting this hypothesis, analysis of cell cycle regulatory genes revealed defective induction of the c-Myc:CUL1 ubiquitin ligase pathway. CUL1 mRNA and protein expression did not increase following IgM ligation on B6 CD22$^{-/-}$ B cells, which corresponded to impaired ubiquitination of cellular proteins (Fig. 6, *A* and *B*). Activation of the c-Myc:CUL1 ubiquitin ligase pathway is necessary for progression from G_1 to S phase of the cell cycle (27). CUL1 is a member of the Cullin family of scaffolding proteins and forms complexes with Skp1 and F-box proteins to form a ternary Skp1-Cullin-F-box (SCF) protein complex (58–60). SCF and SCF-like complexes comprise the largest family of ubiquitin ligases, and regulate the degradation of negative regulatory proteins that maintain cellular senescence, such as the cyclin-dependent kinase inhibitors p27^{Kip1} and p21^{Waf1}, allowing entry into the S phase of the cell cycle (27, 61, 62). Importantly, neither p27^{Kip1} nor p21^{Waf1} expression decreased in B6 CD22$^{-/-}$ B cells following IgM ligation alone, although expression of both molecules decreased in wild-type B cells (Fig. 6*G*). In addition, these proteins were reduced in B6 CD22$^{-/-}$ B cells following costimulation with CD40, correlating with CD40 rescue of proliferation and CUL1 expression in these cells (Figs. 1 and 2). Nevertheless, multiple other molecules may also be targeted by the CUL1 ubiquitin ligase pathway (62, 63), and thus it cannot be ruled out that more complex processes are also involved in CD22 regulation of B cell function via CUL1.

CUL1 expression relies on c-Myc transcriptional activity, and c-Myc-induced CUL1 expression allows exit from the G_1 phase of the cell cycle by promoting SCF complex formation (27). The intensity of c-Myc induction following IgM ligation was markedly impaired in B6 CD22$^{-/-}$ B cells compared to wild-type B cells, especially at latter time points (18 h), where c-Myc protein levels were not increased above that of resting cells (Fig. 6, *C* and *D*). By contrast, reflecting their near-normal capacity to proliferate at optimal concentrations of F(ab′)$_2$ anti-IgM Abs, B6/129 CD22$^{-/-}$ B cells expressed c-Myc and CUL1 at levels similar to wild-type B cells following IgM ligation alone (Fig. 6, *E* and *F*).

Induction of c-Myc expression following IgM ligation on B cells has been reported to require PI 3-kinase activity (37). However, the fact that PI 3-kinase itself was activated in B6 CD22^{-} B cells at levels similar to wild-type B cells (Fig. 5*A*) suggests that a more complex process is involved. Nevertheless, the transient, low-level activation of c-Myc in B6 CD22$^{-/-}$ B cells following IgM stimulation (Fig. 6*C*) provides a mechanism by which these cells may initially begin to increase in size and enter the cell cycle (Fig. 2*C*), but fail to complete the cell cycle and undergo apoptosis as c-Myc levels wane prematurely.

Defective induction of the c-Myc:CUL1 ubiquitin ligase pathway was unique to IgM-ligation, because CD40 ligation alone or in combination with IgM ligation induced c-Myc and CUL1 expression, protein ubiquitination, and p27^{Kip1}/p21^{Waf1} degradation in B6 CD22$^{-/-}$ B cells (Fig. 6). Accordingly, CD40 ligation completely restored IgM-induced lymphoblast development and proliferation in B6 CD22$^{-/-}$ B cell cultures (Figs. 1 and 2). An in vivo role for CD40-mediated rescue of CD22$^{-/-}$ B cells is supported by the observation that germinal center formation was not impaired in B6 CD22$^{-/-}$ mice following immunization with DNP-KLH (Fig. 3, *B* and *C*). These results are also consistent with CD40 engagement rescuing both immature/transitional and chronically activated B cells from BCR-induced cell death (64, 65), by maintaining c-Myc RNA levels (66, 67). Notably, the clonal expansion of B cells following CD40 ligation alone was significantly more robust for both B6 and B6/129 CD22$^{-/-}$ B cells than wild-type B cells (Figs. 1 and 2*A*). Thus, an additional function of CD22 may

be to suppress the activation of B cells through CD40 in the absence of Ag stimulation. In this case, CD22 expression may prevent the inappropriate activation of B cells that are not specific for Ag during ongoing T cell-dependent immune responses in which $CD4^+$ helper T cells express CD154, the ligand for CD40. Because $CD22^{-/-}$ mice generate normal secondary Ab responses (16, 18, 19), isotype-switched (memory) B cells may bypass the need for CD22 expression and rapidly induce c-Myc and CUL1 expression following BCR ligation to more quickly undergo cell division within germinal centers and during recall immune responses. In support of this hypothesis, IgG-expressing B cell lines primarily bypass the CD22-regulatory pathway (68). Together, these data define CD22 and CD40 as the first examples of lymphocyte coreceptors that regulate the c-Myc:CUL1 ubiquitin ligase pathway, which is essential for cellular proliferation.

In summary, the current study reveals that background genes significantly influence the impact of CD22 deficiency on B cell proliferative capacity and cell surface phenotype. The B6/129 mixed genetic background provided proliferative signals that largely compensated for CD22 deficiency, while these signals were mostly absent in the B6 background (Figs. 1 and 2). As such, the differential requirement for CD22 expression in different genetic backgrounds further confirms that lymphocyte coreceptor functions are often dictated by the microenvironment or context in which they are expressed (4). Importantly, progeny from crosses of this line of B6 $CD22^{-/-}$ mice with other mouse lines with B6 genetic backgrounds for additional generations retained the B cell proliferative defect and unique phenotypic characteristics (data not shown), arguing against spontaneous mutations in other genetic loci as the molecular basis for these properties. The impact of the deficiency of other cell surface molecules important in the regulation of B cell function and survival, such as Fas, are also profoundly influenced by genetic background (69, 70). Similarly, genes linked to the *Cd20* locus can influence B cell development (71). Finally, that CD22 function is significantly influenced by background genes in mice suggests that CD22 functional defects in humans may induce more dramatic effects in some individuals than in others regarding altered B cell function and tolerance.

Acknowledgements

We thank Dr. Douglas A. Steeber for critical review of this manuscript, and Melissa Andrews and Isaac Sanford for technical assistance.

References

1. Nemazee, D., and K. Bürki. 1989. Clonal deletion of B lymphocytes in a transgenic mouse bearing anti-MHC class I antibody genes. *Nature 337:562*.
2. Nossal, G. J. V. 1994. Negative selection of lymphocytes. *Cell 76:229*.
3. Rajewsky, K. 1996. Clonal selection and learning in the antibody system. *Nature 381:751*.
4. Tedder, T. F. 1998. Response-regulators of B lymphocyte signaling thresholds provide a context for antigen receptor signal transduction. *Semin. Immunol. 10:259*.
5. Buhl, A. M., and J. C. Cambier. 1997. Co-receptor and accessory regulation of B-cell antigen receptor signal transduction. *Immunol. Rev. 160:127*.
6. Cyster, J. G., and C. C. Goodnow. 1997. Tuning antigen receptor signaling by CD22: integrating cues from antigens and the microenvironment. *Immunity 6:509*.
7. O'Rourke, L., R. Tooze, and D. T. Fearon. 1997. Co-receptors of B lymphocytes. *Curr. Opin. Immunol. 9:324*.
8. Tedder, T. F., J. Tuscano, S. Sato, and J. H. Kehrl. 1997. CD22, a B lymphocyte-specific adhesion molecule that regulates antigen receptor signaling. *Annu. Rev. Immunol. 15:481*.
9. Erickson, L. D., L. T. Tygrett, S. K. Bhatia, K. H. Grabstein, and T. J. Waldschmidt. 1996. Differential expression of CD22 (Lyb8) on murine B cells. *Int. Immunol. 8:1121*.
10. Leprince, C., K. E. Draves, R. L. Geahlen, J. A. Ledbetter, and E. A. Clark. 1993. CD22 associates with the human surface IgM-B cell antigen receptor complex. *Proc. Natl. Acad. Sci. USA 90:3236*.
11. Wilson, G. L., C. H. Fox, A. S. Fauci, and J. H. Kehrl. 1991. cDNA cloning of the B cell membrane protein CD22: a mediator of B-B cell interactions. *J. Exp. Med. 173:137*.
12. Schulte, R. J., M. A. Campbell, W. H. Fischer, and B. M. Sefton. 1992. Tyrosine phosphorylation of CD22 during B cell activation. *Science 258:1001*.
13. Doody, G. M., L. B. Justement, C. C. Delibrias, R. J. Mathews, J. Lin, M. L. Thomas, and D. T. Fearon. 1995. A role in B cell activation for CD22 and the protein tyrosine phosphatase SHP. *Science 269:242*.
14. Chan, V. W. F., C. A. Lowell, and A. L. DeFranco. 1998. Defective negative regulation of antigen receptor signaling in Lyn-deficient B lymphocytes. *Curr. Biol. 8:545*.
15. Poe, J. C., M. Fujimoto, P. J. Jansen, A. S. Miller, and T. F. Tedder. 2000. CD22 forms a quaternary complex with SHIP, Grb2 and Shc: a pathway for regulation of B lymphocyte antigen receptor-induced calcium flux. *J. Biol. Chem. 275:17420*.
16. Nitschke, L., R. Carsetti, B. Ocker, G. Kohler, and M. C. Lamers. 1997. CD22 is a negative regulator of B-cell receptor signalling. *Curr. Biol. 7:133*.
17. O'Keefe, T. L., G. T. Williams, S. L. Davies, and M. S. Neuberger. 1996. Hyperresponsive B cells in CD22-deficient mice. *Science 274:798*.
18. Otipoby, K. L., K. B. Andersson, K. E. Draves, S. J. Klaus, A. G. Farr, J. D. Kerner, R. M. Perlmutter, C.-L. Law, and E. A. Clark. 1996. CD22 regulates thymus-independent responses and the lifespan of B cells. *Nature 384:634*.
19. Sato, S., A. S. Miller, M. Inaoki, C. B. Bock, P. J. Jansen, M. L. K. Tang, and T. F. Tedder. 1996. CD22 is both a positive and negative regulator of B lymphocyte antigen receptor signal transduction: altered signaling in CD22-deficient mice. *Immunity 5:551*.
20. Kelm, S., J. Gerlach, R. Brossmer, C.-P. Danzer, and L. Nitschke. 2002. The ligand-binding domain of CD22 is needed for inhibition of the B cell receptor signal, as demonstrated by a novel human CD22-specific inhibitor compound. *J. Exp. Med. 195:1207*.
21. Jin, L., P. A. McLean, B. G. Neel, and H. H. Wortis. 2002. Sialic acid binding domains of CD22 are required for negative regulation of B cell receptor signaling. *J. Exp. Med. 195:1199*.
22. O'Keefe, T. L., G. T. Williams, F. D. Batista, and M. S. Neuberger. 1999. Deficiency in CD22, a B cell-specific inhibitory receptor, is sufficient to predispose to development of high affinity autoantibodies. *J. Exp. Med. 189:1307*.
23. Sato, S., J. M. Tuscano, M. Inaoki, and T. F. Tedder. 1998. CD22 negatively and positively regulates signal transduction through the B lymphocyte antigen receptor. *Semin. Immunol. 10:287*.
24. Tuscano, J., P. Engel, T. F. Tedder, and J. H. Kehrl. 1996. Engagement of the adhesion receptor CD22 triggers a potent stimulatory signal for B cells and blocking CD22/CD22L interactions impairs T-cell proliferation. *Blood 87:4723*.
25. Tuscano, J. M., P. Engel, T. F. Tedder, A. Agarwal, and J. H. Kehrl. 1996. Involvement of $p72^{syk}$ kinase, $p53/56^{lyn}$ kinase and phosphatidyl inositol-3 kinase in signal transduction via the human B lymphocyte antigen CD22. *Eur. J. Immunol. 26:1246*.
26. Tuscano, J. M., A. Riva, S. N. Toscano, T. F. Tedder, and J. H. Kehrl. 1999. CD22 cross-linking generates B-cell antigen receptor-independent signals that activate the JNK/SAPK signaling cascade. *Blood 94:1382*.
27. O'Hagan, R. C., M. Ohh, G. David, I. M. de Alboran, F. W. Alt, W. G. Kaelin, Jr., and R. A. DePinho. 2000. Myc-enhanced expression of Cull promotes ubiquitin-dependent proteolysis and cell cycle progression. *Genes Dev. 14:2185*.
28. Zhou, L.-J., H. M. Smith, T. J. Waldschmidt, R. Schwarting, J. Daley, and T. F. Tedder. 1994. Tissue-specific expression of the human CD19 gene in transgenic mice inhibits antigen-independent B lymphocyte development. *Mol. Cell. Biol. 14:3884*.
29. Samardzic, T., D. Marinkovic, C.-P. Danzer, J. Gerlach, L. Nitschke, and T. Wirth. 2002. Reduction of marginal zone B cells in CD22-deficient mice. *Eur. J. Immunol. 32:561*.
30. Bikah, G., J. Carey, J. R. Ciallella, A. Tarakhovsky, and S. Bondada. 1996. CD5-mediated negative regulation of antigen receptor-induced growth signals in B-1 B cells. *Science 274:1906*.
31. Norvell, A., L. Mandik, and J. G. Monroe. 1995. Engagement of the antigen-receptor on immature murine B lymphocytes results in death by apoptosis. *J. Immunol. 154:4404*.
32. Tsubata, T., J. Wu, and T. Honjo. 1993. B-cell apoptosis induced by antigen receptor crosslinking is blocked by a T-cell signal through CD40. *Nature 12:645*.
33. Tsubata, T., M. Murakami, and T. Honjo. 1994. Antigen receptor cross-linking induces peritoneal B-cell apoptosis in normal but not autoimmunity-prone mice. *Curr. Biol. 4:8*.
34. Hippen, K. L., L. E. Tze, and T. W. Behrens. 2000. CD5 maintains tolerance in anergic B cells. *J. Exp. Med. 191:883*.
35. Loder, F., B. Mutschler, R. J. Ray, C. J. Paige, P. Sideras, R. Torres, M. C. Lamers, and R. Carsetti. 1999. B cell development in the spleen takes place in discrete steps and is determined by the quality of B cell receptor-derived signals. *J. Exp. Med. 190:75*.
36. Donahue, A. C., and D. A. Fruman. 2003. Proliferation and survival of activated B cells requires sustained antigen receptor engagement and phosphoinositide 3-kinase activation. *J. Immunol. 170:5851*.
37. Grumont, R. J., A. Strasser, and S. Gerondakis. 2002. B cell growth is controlled by phosphatidylinositol 3-kinase-dependent induction of Rel/NF-κB regulated c-*myc* transcription. *Mol. Cell 10:1283*.
38. Yohannan, J., J. Wienands, K. M. Coggeshall, and L. B. Justement. 1999. Analysis of tyrosine phosphorylation-dependent interactions between stimulatory effector proteins and the B cell co-receptor CD22. *J. Biol. Chem. 274:18769*.
39. Franke, T. F., S.-I. Yang, T. O. Chan, K. Datta, A. Kazlauskas, D. K. Morrison, D. R. Kaplan, and P. N. Tsichlis. 1995. The protein kinase encoded by the *Akt* proto-oncogene is a target of the PDGF-activated phosphatidylinositol 3-kinase. *Cell 81:727*.

40. Burgering, B. M. T., and P. J. Coffer. 1995. Protein kinase B (c-*akt*) in phosphatidylinositol 3-kinase signal transduction. *Nature 376:599*.
41. Javad Aman, M., T. D. Lamkin, H. Okada, T. Kurosaki, and K. S. Ravichandran. 1998. The inositol phosphatase SHIP inhibits Akt/PKB activation in B cells. *J. Biol. Chem. 273:33922*.
42. Alessi, D. R., M. Andjelkovic, B. Caudwell, P. Cron, N. Morrice, P. Cohen, and B. A. Hemmings. 1996. Mechanism of activation of protein kinase B by insulin and IGF-1. *EMBO J. 15:6541*.
43. Datta, R. S., H. Dudek, X. Tao, S. Masters, H. Fu, Y. Gotoh, and M. E. Greenberg. 1997. Akt phosphorylation of BAD couples survival signals to the cell-intrinsic death machinery. *Cell 91:231*.
44. Zha, J., H. Harada, E. Yang, J. Jockel, and S. J. Korsmeyer. 1996. Serine phosphorylation of death agonist BAD in response to survival factor results in binding to 14-3-3 not Bcl-x_L. *Cell 87:619*.
45. Yang, E., J. Zha, J. Jockel, L. H. Boise, C. B. Thompson, and S. J. Korsmeyer. 1995. Bad, a heterodimeric partner for Bcl-x_L and Bcl-2, displaces Bax and promotes cell death. *Cell 80:285*.
46. Healy, J. I., R. E. Dolmetsch, L. A. Timmerman, J. G. Cyster, M. L. Thomas, G. R. Crabtree, R. S. Lewis, and C. C. Goodnow. 1997. Different nuclear signals are activated by the B cell receptor during positive versus negative signaling. *Immunity 6:419*.
47. Romashkova, J. A., and S. S. Makarov. 1999. NF-κB is a target of AKT in anti-apoptotic PDGF signaling. *Nature 401:86*.
48. Wang, C. Y., M. W. Mayo, R. G. Korneluk, D. V. Goeddel, and A. S. J. Baldwin. 1998. NF-κB anti-apoptosis: induction of TRAF1 and TRAF2 and c-IAP1 and c-IAP2 to suppress caspase-8 activation. *Science 281:1680*.
49. Ozes, O. N., L. D. Mayo, J. A. Gustin, S. R. Pfeffer, L. M. Pfeffer, and D. B. Donner. 1999. NF-κB activation by tumour necrosis factor requires the Akt serine-threonine kinase. *Nature 401:82*.
50. Adams, J. M., A. W. Harris, C. A. Pinkert, L. M. Corcoran, W. S. Alexander, S. Cory, R. D. Palmiter, and R. L. Brinster. 1985. The c-*myc* oncogene driven by immunoglobulin enhancers induces lymphoid malignancy in transgenic mice. *Nature 318:533*.
51. Shirane, M., Y. Harumiya, N. Ishida, A. Hirai, C. Miyamoto, S. Hatakeyama, K. Nakayama, and M. Kitagawa. 1999. Down-regulation of $p27^{Kip1}$ by two mechanisms, ubiquitin-mediated degradation and proteolytic processing. *J. Biol. Chem. 274:13886*.
52. Yu, Z. K., J. L. Gervais, and H. Zhang. 1998. Human CUL-1 associates with the SKP1/SKP2 complex and regulates p21(CIP1/WAF1) and cyclin D proteins. *Proc. Natl. Acad. Sci. USA 95:11324*.
53. Otipoby, K. L., K. E. Draves, and E. A. Clark. 2001. CD22 regulates B cell receptor-mediated signals via two domains that independently recruit Grb2 and SHP-1. *J. Biol. Chem. 276:44315*.
54. King, L. B., and J. G. Monroe. 2000. Immunobiology of the immature B cell: plasticity in the B-cell antigen receptor-induced response fine tunes negative selection. *Immunol. Rev. 176:86*.
55. Qian, Y., C. Santiago, M. Borrero, T. F. Tedder, and S. H. Clarke. 2001. Lupus-specific antiribonucleoprotein B cell tolerance in nonautoimmune mice is maintained by differentiation to B-1 and governed by B cell receptor signaling thresholds. *J. Immunol. 166:2412*.
56. Goodnow, C. C., J. Crosbie, H. Jorgensen, R. A. Brink, and A. Basten. 1989. Induction of self-tolerance in mature peripheral B lymphocytes. *Nature 342:385*.
57. Sato, S., D. A. Steeber, P. J. Jansen, and T. F. Tedder. 1997. CD19 expression levels regulate B lymphocyte development: human CD19 restores normal function in mice lacking endogenous CD19. *J. Immunol. 158:4662*.
58. Lisztwan, J., A. Marti, H. Sutterluty, M. Gstaiger, C. Wirbelauer, and W. Krek. 1998. Association of human CUL-1 and ubiquitin-conjugating enzyme CDC34 with the F-box protein $p45^{SKP2}$: evidence for evolutionary conservation in the subunit composition of the CDC34-SCF pathway. *EMBO J. 17:368*.
59. Lyapina, S. A., C. C. Correll, E. T. Kipreos, and R. J. Deshaies. 1998. Human CUL1 forms an evolutionarily conserved ubiquitin ligase complex (SCF) with SKP1 and an F-box protein. *Proc. Natl. Acad. Sci. USA 95:7451*.
60. Michel, J. J., and Y. Xiong. 1998. Human CUL-1, but not other cullin family members, selectively interacts with SKP1 to form a complex with SKP2 and cyclin A. *Cell Growth Differ. 9:435*.
61. Dealy, M. J., K. V. Nguyen, J. Lo, M. Gstaiger, W. Krek, D. Elson, J. Arbeit, E. T. Kipreos, and R. S. Johnson. 1999. Loss of Cull results in early embryonic lethality and dysregulation of cyclin E. *Nat. Genet. 23:245*.
62. Zheng, N., B. A. Schulman, L. Song, J. J. Miller, P. D. Jeffrey, P. Wang, C. Chu, D. M. Koepp, S. J. Elledge, M. Pagano, et al. 2002. Structure of the Cull-Rbx1-Skp1-F box^{Skp2} SCF ubiquitin ligase complex. *Nature 416:703*.
63. Maniatis, T. 1999. A ubiquitin ligase complex essential for the NF-κB, Wnt/Wingless, and Hedgehog signaling pathways. *Genes Dev. 13:505*.
64. Eris, J. M., A. Basten, R. Brink, K. Doherty, M. R. Kehry, and P. D. Hodgkin. 1994. Anergic self-reactive B cells present self antigen and respond normally to CD40-dependent T-cell signals but are defective in antigen-receptor-mediated functions. *Proc. Natl. Acad. Sci. USA 91:4392*.
65. Sater, R. A., P. C. Sandel, and J. G. Monroe. 1998. B cell receptor-induced apoptosis in primary transitional murine B cells: signaling requirements and modulation by T cell help. *Int. Immunol. 10:1673*.
66. Soebelt, F., I. Berberich, G. Shu, E. Serfling, and E. A. Clark. 1997. Role for CD40-mediated activation of c-Rel and maintenance of c-myc RNA levels in mitigating anti-IgM-induced growth arrest. *Cell. Immunol. 181:13*.
67. Wu, M., W. Yang, R. E. Bellas, S. L. Schauer, M. J. FitzGerald, H. Lee, and G. E. Sonenshein. 1997. c-*myc* promotes survival of WEHI 231 B lymphoma cells from apoptosis. *Curr. Top. Microbiol. Immunol. 224:91*.
68. Wakabayashi, C., T. Adachi, J. Wienands, and T. Tsubata. 2002. A distinct signaling pathway used by the IgG-containing B cell antigen receptor. *Science 298:2392*.
69. Izui, S., V. E. Kelley, K. Masuda, H. Yoshida, J. B. Roths, and E. D. Murphy. 1984. Induction of various autoantibodies by mutant gene *lpr* in several strains of mice. *J. Immunol. 133:227*.
70. Kelley, V. E., and J. B. Roths. 1985. Interaction of mutant *lpr* gene with background strain influences renal disease. *Clin. Immunol. Immunopathol. 37:220*.
71. O'Keefe, T. L., G. T. Williams, S. L. Davies, and M. S. Neuberger. 1998. Mice carrying a CD20 gene disruption. *Immunogenetics 48:125*.